

Studies on Synthesis, Characterization, and Metal Adsorption of Mimosa and Valonia Tannin Resins

Mahmut Özacar,¹ Cengiz Soykan,² İ. Ayhan Şengil³

¹Department of Chemistry, Science and Arts Faculty, Sakarya University, 54100 Sakarya-Turkiye

²Department of Chemistry, Yozgat Science and Arts Faculty, Erciyes University, 66100 Yozgat-Turkiye

³Department of Environmental Engineering, Engineering Faculty, Sakarya University, 54040 Sakarya-Turkiye

Received 2 March 2005; revised 23 May 2005; accepted 1 December 2005

DOI 10.1002/app.23944

Published online in Wiley InterScience (www.interscience.wiley.com).

ABSTRACT: A few thermosetting wood adhesive tannin resin system from formaldehyde reaction with both condensed and hydrolysable tannin has been developed. Polymerization of formaldehyde with mimosa tannin and valonia tannin was carried out at optimal conditions obtained from literature to establish the adhesive resin formulation. Formed reaction products were characterized by FTIR spectroscopy. The possible adsorption mechanisms for the adsorption of various metal ions onto tannin-formaldehyde

resins were proposed. Also, thermal analysis were studied and discussed by differential scanning calorimetry and thermogravimetry. © 2006 Wiley Periodicals, Inc. *J Appl Polym Sci* 102: 786–797, 2006

Key words: mimosa and valonia tannin; formaldehyde reaction; adsorption mechanism; FTIR spectroscopy; thermal analysis

INTRODUCTION

Tannin compounds, extracted from the wood, bark, leaves, fruits, and galls of plants, are unique and inexpensive natural materials. Depending on their structure, they can be classified in two main categories: hydrolysable and condensed tannins, and they are widely distributed in nature. They have multiple adjacent polyhydroxyphenyl groups in their chemical structure, which have extremely high affinity for proteins, metal ions, and other macromolecules like polysaccharides.^{1,2} Tannins have been a subject of extensive research leading to the development of a wide range of industrial applications. These include use in tanneries, wood adhesives, manufacture of inks, dyeing of textiles, flocculant for water treatment, corrosion inhibitor for steels, dispersants, antioxidants, medicine, cosmetic, etc.^{3–7} Following the oil crisis of the 1970s, interest in plant-based polymeric resins increased, and significant research developments on the tannin-based resins were achieved in South America, Australia, and South Africa.^{3,4}

This article will describe how tannin-formaldehyde resin can be prepared and characterized to use as an adsorbent for the removal of various heavy metals. When tannin compounds are used as an adsorbent, however, they easily dissolve in water. To overcome

this shortcoming, and to enhance adsorption capacity, various chemical attempts tried have been cited in elsewhere.¹ In this study, possible reaction mechanisms of formaldehyde with both condensed and hydrolysable tannin have been discussed. Formed reaction products were characterized by FTIR spectroscopy, since FTIR spectroscopy offers a unique capability in terms of the conversion of a specific functional group. In particular, the appearance of the hydroxyl group, methylol group, and dimethylene ether bridges can be easily monitored.⁸ Thermal analysis techniques have often been used to study and interpret the curing of thermostable adhesives and their kinetics. Curing rate is affected, apart from formulation,⁹ by the synthesis procedure¹⁰ and by the presence of catalysts and other additives.¹¹ Curing characteristics can affect resin properties such as stability, spreading and wood penetration capacity, fragility after curing, etc., thus conditioning its use in the factory. Even if dynamomechanical analysis (DMA) has been used to study curing from the point of view of its mechanical behavior,¹² the difficulty in modeling the process has oriented most curing studies toward the use of differential scanning calorimetry (DSC) and thermogravimetry (TG). The measurements of an extensive property such as the enthalpy in DSC does not allow its changes to be evaluated separately in function of the contributions of the simple reactions that take place. For this reason, DSC cannot be used to analyze the different reactions that take place during thermal transformation, especially in adhesive curing. The main advantages of these polymeric resins are

Correspondence to: C. Soykan (soykan@erciyes.edu.tr).

high chemical and mechanical stability. These materials have now been used for over 20 years as industrial thermosetting tannin-formaldehyde adhesives for wood products.¹³ Also, the possible adsorption mechanisms for the adsorption of various metal ions onto tannin-formaldehyde resins were proposed.

MATERIALS AND METHODS

Materials

Two types of commercial tannin extracts, mimosa and valonia, were obtained from Tuzla Dericiler Sanayi Sitesi, İstanbul-Türkiye. The tannin content of the extracts were determined to be 63% as flavanoid for mimosa tannin and 70% as gallotannin for valonia tannin, according to the Vanilin-test,¹⁴ the Prussian Blue-test,¹⁵ and the Rhodanine-test.¹⁶ The extracts, which are considered their tannin contents were used in the polymerization experiments without further purification. All other chemicals used in the studies were of analytical grade and obtained from Merck Chemical (Turkey).

Preparation of mimosa tannin resin

Commercial extract (12.70 g; 8 g of mimosa tannin or equivalent 2.76×10^{-2} mol) was dissolved in 50 mL of distilled water. A 65 mL of formaldehyde aqueous solution having 37% by weight of formaldehyde (0.874 mol) was added and mixed for 5 min. Then 15 mL of aqueous ammonia solution at 13.3N (0.200 mol) was added to the solution to precipitate a tannin compound. It is preferable that the pH of the solution after the addition of ammonia is no less than 7. If it is less than pH 7, tannin does not precipitate. After the addition of ammonia, brown precipitate was formed. The mixture containing the precipitate was stirred at 313 K for 35 min to complete the crosslinking reaction. Subsequently, precipitated tannin thus produced was separated by filtration. Resin particles obtained were washed by distilled water to away unreacted substances. The condensed tannin resin (CTR) was sieved to give different particle size fractions using ASTM standard sieves, and 75–100 μm particle size and dried at 343 K for 24 h and then kept for following experiments.

Preparation of valonia tannin resin

Commercial valonia extract powder (11.45 g) corresponding to a hydrolysable tannin powder (8 g or 6.80×10^{-3} mol of gallotannin) was added to 50 mL of 13.3N (0.665 mol) aqueous ammonia, followed by stirring for 5 min to dissolve it. To the resulting solution was added 65 mL of an aqueous solution containing 37% formaldehyde (0.874 mol), followed by stirring

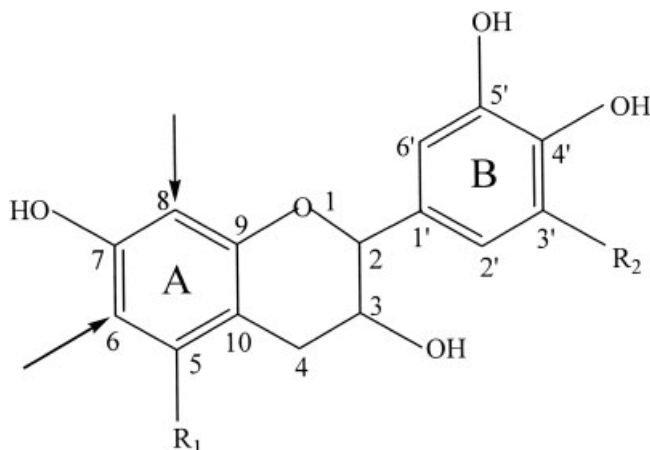
for 5 min for uniform mixing. When this stirring was stopped, a yellow precipitate formed. After the resulting liquid containing the precipitate was stirred for 30 min, the stirred liquid was filtered through filter paper. The precipitate thus obtained was added to 50 mL distilled water, and heated at 343 K for 3 h with stirring to remove free formaldehyde. The heated liquid was filtered. Subsequently, the precipitate thus obtained was added to 100 mL of 0.1N HNO_3 , followed by stirring for 30 min. The liquid containing the precipitate is mixed with mineral acid such as nitric, hydrochloric, and sulfuric acid to make the precipitate insoluble in acidic and basic medium. Finally, the HNO_3 solution was filtered and washed with distilled water, followed by drying the filtered precipitate at 353 K to thereby obtain an insoluble tannin resin. The hydrolysable tannin resin (HTR) was sieved to give different particle size fractions using ASTM standard sieves, and 75–100 μm particle size was used in the adsorption experiments.

Adsorption studies

The lead, copper, zinc, and cadmium solutions were prepared by dissolving $\text{Pb}(\text{NO}_3)_2$, $\text{CuSO}_4 \cdot 5\text{H}_2\text{O}$, $3\text{CdSO}_4 \cdot 8\text{H}_2\text{O}$, and $\text{ZnSO}_4 \cdot 7\text{H}_2\text{O}$, respectively, in distilled water at 100 mg/L concentrations. Adsorption experiments were carried out by agitating 1 L of each metal ion solution with 1 g mimosa tannin resin (MTR) or valonia tannin resin (VTR) at pH 4 and at room temperature (298 ± 2 K). When the initial pH of the adsorption medium was adjusted to a higher value of pH 4, some of the metals were precipitated due to the existence of OH^- ions in the adsorption medium. The mixture was continuously agitated by a jar test apparatus at 150 rpm for 3 h. At the end of the adsorption period, the solutions were filtered through a 0.45 μm Milipore filter paper. All metal concentrations were measured using AAS equipped with an auto-sampler (Shimadzu AA6701F). The amounts of metal adsorbed were calculated from the concentrations in solutions before and after adsorption process.

Measurements

FTIR spectra were recorded on a Mattson Intensity Series FTIR spectrophotometer. The samples were prepared after removing the supernatant, and a portion of the residue was filtered through 0.45 μm Millipore membrane filters. The remaining portion was dried at 353 K for 4 h. Potassium bromide disks were prepared by mixing 1 mg of these samples with 200 mg of KBr (spectrometry grade) at 10,000 kg/cm² pressure for 30 min under vacuum. The spectra were recorded from 4000 to 400 cm^{-1} (100 scans) on samples in KBr disks. Thermal analysis were carried out by using a Setaram Labsys TGA thermobalance and Setaram DSC-131.



Scheme 1 The flavanoid unit in mimosa tannin. A-ring: $R_1 = \text{H}$ for resorcinol and $R_1 = \text{OH}$ for phloroglucinol; B-ring: $R_2 = \text{H}$ for pyrocatechol and $R_2 = \text{OH}$ for pyrogallol.

Samples of 5–8 mg held in alumina open crucibles, were used and their weights were measured as a function of temperature and stored in the list of data of the appropriate built-in program of the processor. The TGA curves were immediately printed at the end of each experiment and the weights of the sample were then transferred to a PC at various temperatures.

RESULTS AND DISCUSSION

Tannin-formaldehyde reactions

Tannins are made up of complex phenolic compounds of high molecular weight, ranging from 500 to 20,000. They are divided into two major groups: (a) condensed tannins (proanthocyanidins) and (b) hydrolyzable tannins (polyesters based on gallic and/or ellagic acid and their derivatives). Generally, tannins are soluble in water, with exception of some very high molecular weight compounds.¹⁷

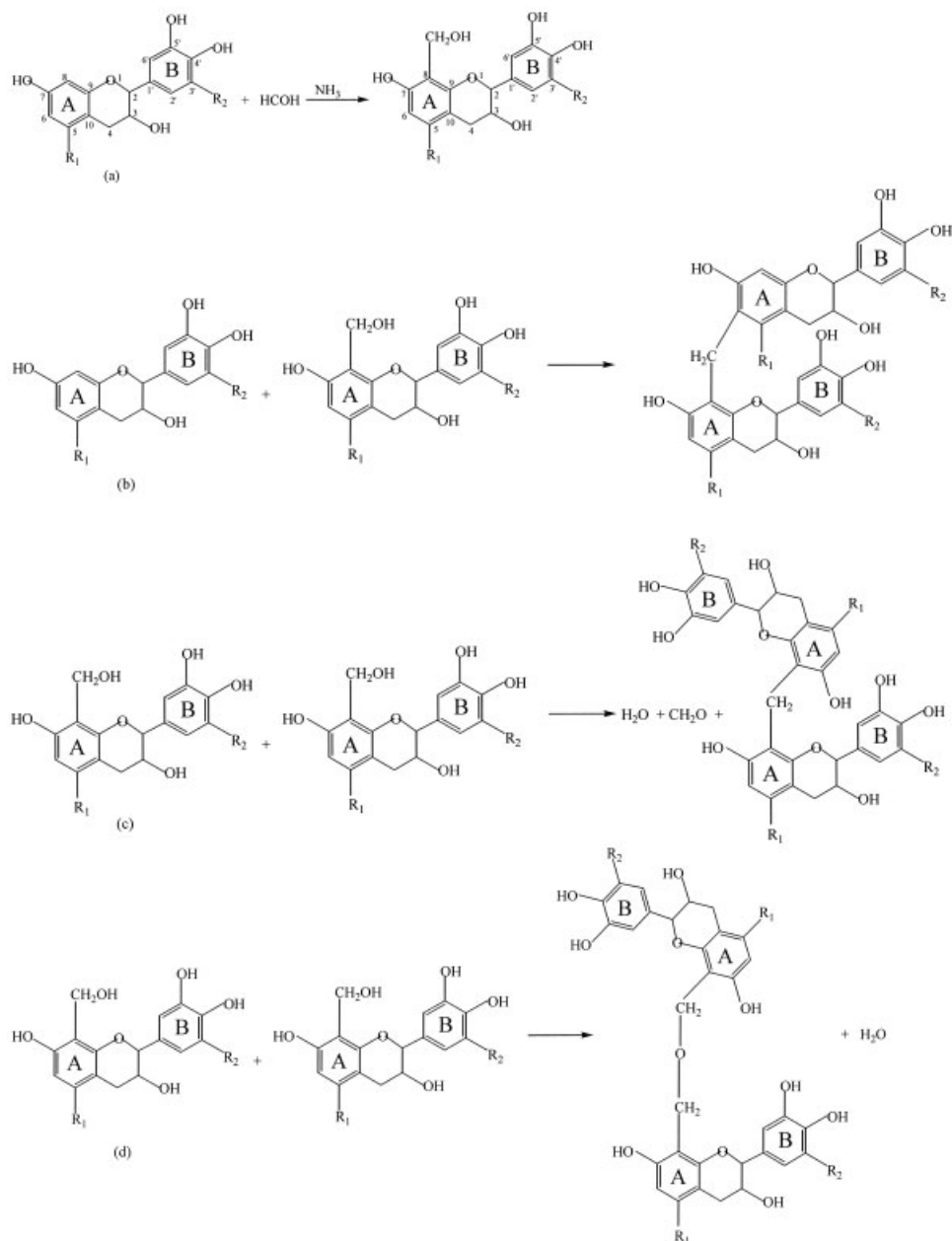
Mimosa tannin (MT) is condensed tannin that has a polymeric structure containing on the average four flavanoid units. They are not an isolated group of compounds, but a part of the vast collection of natural compounds, and chemicals based on flavan-3-ol units. The percentage of flavanoid units in mimosa tannin (Scheme 1) is approximately: resorcinol (A)-pyrogallol (B) 56%, resorcinol (A)-pyrocatechol (B) 24%, phloroglucinol (A)-pyrogallol (B) and phloroglucinol (A)-pyrocatechol (B) 20%.^{18,19} A-rings of mimosa tannin serve as very reactive nucleophiles and B-rings provide antioxidant properties and excellent sites for complexation with metals and biopolymers due to the presence of ortho-hydroxyls.^{18,19}

The nucleophilic centers on the A-ring of a flavanoid unit tend to be more reactive than those on the B-ring. This is due to the vicinal hydroxyl substituents, which merely cause general activation in the B-ring

without any localized effects such as those found in the A-ring. Formaldehyde reacts with tannins to produce polymerization through methylene bridge linkages at reactive positions on the flavanoid molecules, mainly the A-rings. Therefore, in all industrially meaningful tannin-formaldehyde resins developed until now, only the highly reactive resorcinolic A-rings of the flavanoids were utilized, the catecholic or pyrogalloic B-rings presenting such a low reactivity only in extreme conditions of pH, time, and temperature would be able to condense with formaldehyde.^{20,21} Pizzi stated that while catecholic or pyrogalloic B-rings of the flavanoid unit do not react with formaldehyde at pH lower than 10, the addition of divalent and trivalent metallic ions such as zinc acetate to the reaction mixture induce the B-rings to react with formaldehyde at lower pHs, the optimum being in the pH 4.5–5.5 range.^{22,23}

Alkaline-catalyzed phenolic resins are called resoles. Tannin, being phenolic, reacts with formaldehyde in a manner similar to that for the reaction of formaldehyde with phenol. However, unlike most synthetic phenolic compounds, tannin has a high reactivity toward formaldehyde, and is larger in size. The free C6 or C8 sites on the A-ring react with formaldehyde, due to their strong nucleophilicity, to form the insoluble tannin. This high reactivity of tannins toward formaldehyde is the result of their A-ring phloroglucinolic or resorcinolic nuclei, which have 10- to 50-times higher rate of reaction than the reaction of phenol with formaldehyde. Therefore, during the condensation reaction of tannin with formaldehyde, tannin-formaldehyde resoles become rapidly immobilized due to premature gelation as a result of its high reactivity and molecular size.²⁴ There are two steps leading to formation of tannin-formaldehyde resole resins: methylation and condensation reactions. The first step, methylation, is an electrophilic aromatic substitution reaction and, consequently, the products obtained will be substituted in ortho and para positions. The presence of a second or third activating group as in the case of resorcinol or phloroglucinol (Scheme 1) will activate even more the original phenol.¹¹ The second step is a condensation reaction, where a methylol group of one molecule reacts with a second tannin, releasing a water molecule, thus forming a methylene linkage. Further condensations result in polymerization to obtain the resole.¹¹ The methylation and condensation reactions are shown in Scheme 2.

The original approach that each crosslinking node is formed from three chains joining is not strictly valid in the case of the reaction of tannins with formaldehyde. This approach is valid strictly if one considers the tannin as composed of monomers presenting three available reactive sites, namely, C6 and C8 being re-

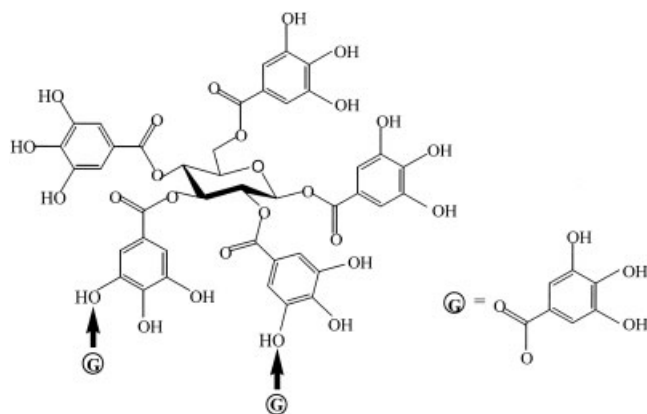


Scheme 2 Formation of mimosa tannin-formaldehyde resin. (a) methylation reaction of flavanoid unit in mimosa tannin; (b–d) condensation reaction path of flavanoid unit in mimosa tannin.

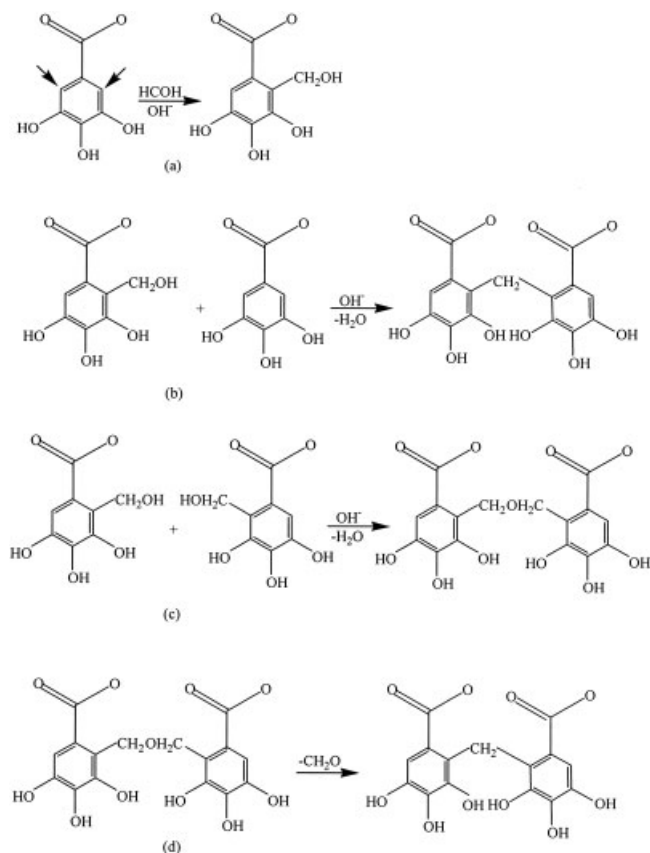
active with formaldehyde and C4 joining directly with another flavanoid unit.²⁵

The process of crosslinking is complicated in the case of tannin, whereas resol resin produces linear and regular crosslinking. This is due to the structure and high molecular weight of tannin. Furthermore, in the case of tannin, some of the —OH groups do not participate in the crosslink formations. Apart from resol resin, tannin molecules show steric hindrance for —OH groups interactions because of their branched complex structure.⁸

Turkish gallo-tannin (valonia tannin) is hexa-(or hepta)-O-galloyl- β -D-glucose,^{25–27} and its structure is shown in Scheme 3.



Scheme 3 Gallotannin structure in valonia tannin.



Scheme 4 Reaction of galloyl group in valonia tannin with formaldehyde. (a) methylation reaction of galloyl unit in valonia tannin; (b–d) condensation reaction path of galloyl unit in valonia.

Galloyl group in the gallotannin (Scheme 3) consists of an aromatic ring bearing a esterified carboxyl group (position 1) and three adjacent hydroxyl groups (positions 3, 4, and 5), leaving two free sites on the ring. Reactivity considerations show that the hydroxyl functions in 3 and 5 activate the free positions, while the remaining groups deactivate them. The overall effect is that galloyl group possesses an enhanced reactivity toward electrophilic aromatic substitution, compared to phenol, while not being as reactive as phloroglucinol.¹¹

VTR formation reactions are shown in Scheme 4. There are two possible condensation reaction paths for the reaction of gallotannin (valonia tannin) and formaldehyde, leading to the formation of a methylene bridge. The first step of two mechanisms, methylation, is an electrophilic aromatic substitution reaction [Scheme 4(a)]. The second step is a condensation reaction. The two mechanism involve a hydroxymethyl group with either a proton of the aromatic ring (ortho position), with the release of one molecule of water [Scheme 4(b)], or a hydroxymethyl group with the simultaneous release of one molecule of water and one molecule of formaldehyde [Scheme 4(c)]. In both

cases, a methylene bridge is created. Thus, the formaldehyde reaction at the ortho position of a sufficiently large number of galloylated rings of valonia tannin, would open the door to the formation of a three dimensional structure (crosslinking) upon reaction conditions. This type of network is generally regarded as the best resin system.^{11,28}

As the MT and VT dissolve in water, both of them do not dissolve in water after the reaction of tannins with formaldehyde. Thus, insoluble MTR and VTR formed by the reaction of tannins with formaldehyde show a perfect adsorbent properties for the adsorption of many metal ions and unwanted compounds from aqueous solutions.

FTIR spectroscopy studies

The FTIR spectra of MT, MTF resin, and various metal-adsorbed MTF resin are shown in Figure 1. Generally, wide bands in the range of 3550–3100 cm⁻¹ correspond to —OH bridging groups in all systems and are attributed to water molecules hydrogen-bonded with —OH groups in the MTR particles. The small peaks in the region of 2880–2940 cm⁻¹ are associated with the methylene (—CH₂—) bridges of the tannin-formaldehyde resins.^{8,28,29} It has been demonstrated that a large number of methylene ether bridges (—CH₂—O—CH₂—) occur, which rearrange themselves with relative ease to form methylene (—CH₂—) bridges with the release of formaldehyde.³⁰ Also, C—H stretching vibrations in the benzene rings give absorption bands in this region. The absorption bands between 1621 and 1463 cm⁻¹ are characteristic of the elongation of the aromatic —C=C— bonds. The deformation vibration of the carbon–carbon bonds in the phenolic groups absorbs in the region of 1500–1400 cm⁻¹. The peak around 1250 cm⁻¹ is associated with the —CO stretchings of the benzene ring and the dimethylene ether bridges formed by reaction with the formaldehyde. The peaks at 1100–1010 cm⁻¹ in the spectrum of MT are due to C—O stretching and CH deformation.

The spectra of MTF resin were compared with the IR spectrum of the MT. The intensity of C—O peak at 1010 cm⁻¹ is increased and broadened region of 1100–960 cm⁻¹. Also, the broad peaks in the spectra of MTF resin at this region may be attributed to the formation of dimethylene ether (—CH₂—O—CH₂—) linkage. Since the most characteristic absorption of aliphatic ethers is a strong band in the 1150–1085 cm⁻¹ region due to asymmetrical C—O—C stretching, this band usually occurs near 1125 cm⁻¹.³¹ The deformation vibrations of the C—H bond in the benzene rings give absorption bands in the 840–730 cm⁻¹ range. This group does not participate in any chemical reaction during the polymerization. However, this peak

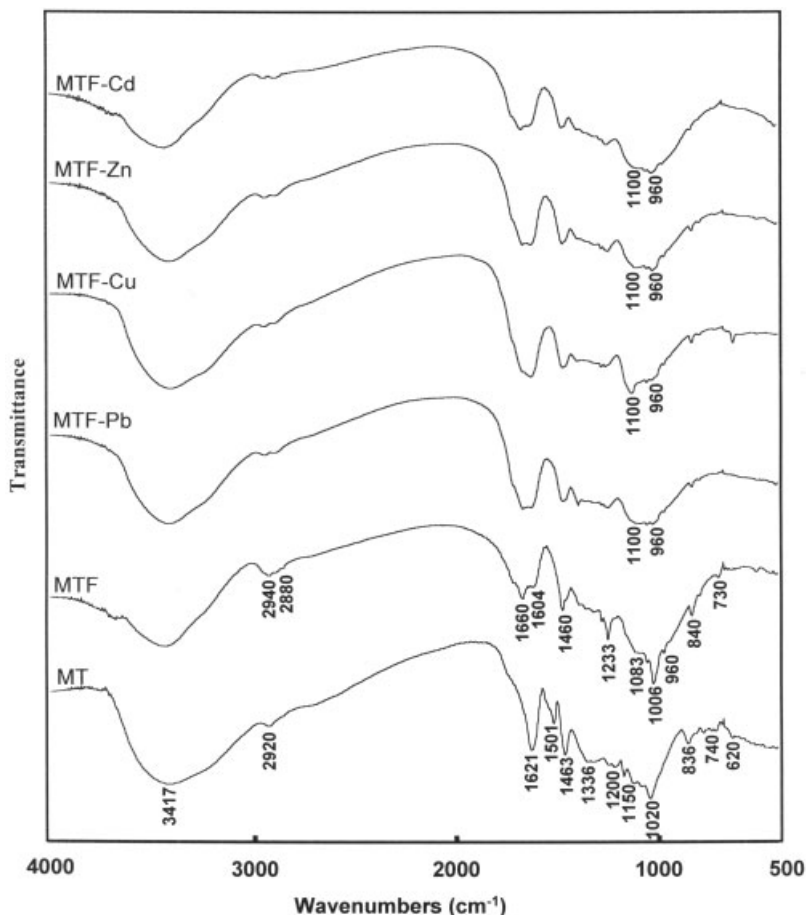


Figure 1 FTIR spectra of metal ions adsorbed onto MTR. MT: mimosa tannin; MTF: mimosa tannin-formaldehyde resin; MTF-Pb: Pb^{2+} -adsorbed mimosa tannin-formaldehyde resin; MTF-Cu: Cu^{2+} -adsorbed mimosa tannin-formaldehyde resin; MTF-Zn: Zn^{2+} -adsorbed mimosa tannin-formaldehyde resin; MTF-Cd: Cd^{2+} -adsorbed mimosa tannin-formaldehyde resin.

showed a gradual decrease as the process of polymerization progressed, because when the reaction takes place, the volume of the system contracts.^{8,29}

The spectra of MTF-metal adsorbed resins were compared with the IR spectra of the MT and MTF resin. The peak of methylol group (C—O) at the region of 1100–960 cm^{-1} in the spectra of MTF-metal adsorbed resins is more broadened than those of MTF and MT spectra. These changes at MTF-metal adsorbed resins are attributed to complexation of MTF resins and metal ions.³²

Figure 2 presents the FTIR spectra of VT, VTF, and various metal-adsorbed VTF resin systems. The broad peak in the region of 3550–3100 cm^{-1} is characteristic of the —OH stretchings of the phenolic and methylol group of tannin. In all spectra, the small peaks in near the 2900 cm^{-1} are due to aromatic C—H stretching vibrations.^{8,31}

The band at 1732 cm^{-1} in the spectrum of VT belongs to carboxyl-carbonyl groups. The absorption bands between 1604 and 1444 cm^{-1} are related to aromatic —C=C— bonds. The peaks at 1315 and 1037 cm^{-1} in the spectrum of tannin belong to phenol

groups.^{28,29} The peak at 1160 cm^{-1} is due to aromatic C—H deformation.⁸ The deformation vibrations of the C—H bond in the benzene rings also give small absorption bands in the 910–740 cm^{-1} range.

When the spectra of VTF resin were compared with the IR spectrum of the VT, the peaks at 1732 and 1604 cm^{-1} belonging to C=O and —C=C— are combined and broadened. This broad peak is located at 1671 cm^{-1} with a shoulder at 1604 cm^{-1} , which may be attributed to the —C=C— stretching vibration. This change occurs most probably due to environmental change of C=O groups of VTF, since the formation of methylene bridge in ortho position of C=O groups of VT during the polymerization process will affect the vibration of C=O group. The band intensities between 1315 and 1037 cm^{-1} are reduced and slightly shifted in the spectrum of the VTF resin. Also, the peaks at 1315 and 1037 cm^{-1} region are converted to small peak series. This situation may be attributed to the —CO stretchings of benzene ring and the phenolic —OH groups. Also, the formation of —CH₂—O—CH₂— linkage appeared at 1150–1085 cm^{-1} .³¹ The intensity of peak at about 1450 cm^{-1} is slightly in-

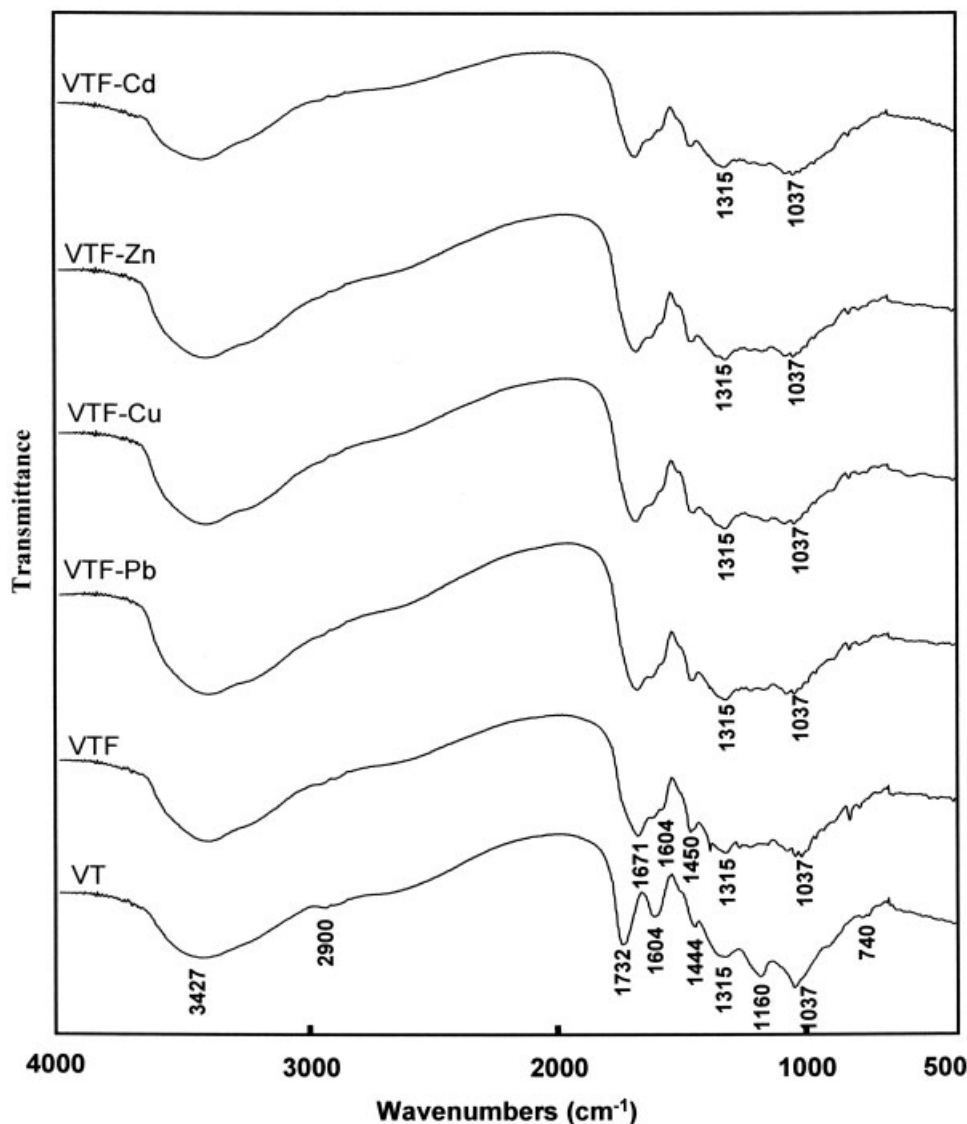


Figure 2 FTIR spectra of metal ions adsorbed onto VTR. VT: valonia tannin; VTF: valonia tannin-formaldehyde resin; VTF-Pb: Pb^{2+} -adsorbed valonia tannin-formaldehyde resin; VTF-Cu: Cu^{2+} -adsorbed valonia tannin-formaldehyde resin; VTF-Zn: Zn^{2+} -adsorbed valonia tannin-formaldehyde resin; VTF-Cd: Cd^{2+} -adsorbed valonia tannin-formaldehyde resin.

creased due to the formation of methylene bridges by reaction with the formaldehyde.^{28,29}

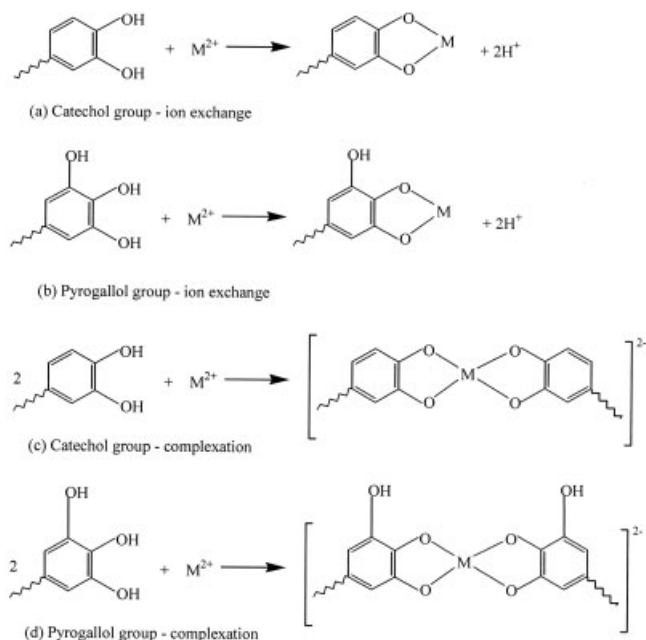
When the spectra of various metal-adsorbed VTF resins were compared with VTF resin, the small peak series at 1315 and 1037 cm^{-1} are combined and shifted, respectively, because of metal-tannate complex formation between various metal ions and some phenolic groups of tannin.^{33–36}

It is expected that the change in the wide hydroxyl band 3550–3100 cm^{-1} region in the spectra of both MTF- and VTF-metal adsorbed resins after the complexation or ion exchange reactions between various metal ions and phenolic groups of both tannin resins. But these changes are observed at 1100–960 cm^{-1} and 1315–1037 cm^{-1} regions for the spectra of MTF- and VTF-metal adsorbed resins, respectively, because all

of the —OH groups in the tannin resins do not participate in the complexation or ion exchange reactions between the tannin resins and metal ions (see Scheme 5). The phenolic groups participated complexation or ion exchange reactions are located in the 1100–960 cm^{-1} region for MTF and in the 1315–1037 cm^{-1} region for VTF resins. The wide bands in the 3550–3100 cm^{-1} region are belonging to free hydroxyl groups (not participate reactions with metal ions) of the both tannin resins.

Thermal studies

The thermal stabilities of the MTR and VTR were investigated by thermogravimetric analysis (TGA) in a nitrogen stream at a heating rate of 10°C min^{-1} . The



Scheme 5 Adsorption mechanisms for adsorption of divalent metal ion onto MTR and VTR.

thermal curves of both recovered tannin are shown in Figure 3. The decomposition of these systems essentially occurs in three stages.³⁷ The first stage covers the postcuring, thermal reforming, and preliminary oxidation steps. The second stage depends mainly on the

stripping of the ring, chain cleavage, and elimination of volatile fractions. In the third stage, oxidative degradation takes place at markedly higher temperatures.

TGA curves of VTR show these three stages. The first stage corresponds to the elimination of water, in which a nearly 9% weight loss has occurred, while in the second stage, the decomposition temperature range of 150–300°C could be the result of the partial breakdown of the intermolecular bonding and the 28% weight loss that has already occurred. The third stage occurs in the temperature range of 300–750°C, which may be due to the fragmentation of the intramolecular forces, and the molecule as a whole is decomposed with 40% weight loss. The char yield was nearly 25%, which accounts for the elements present in the wastewater.

The TGA trace of MTR impregnate shows its three stages of decomposition. In the initial stage of decomposition, nearly 6% weight loss occurred, which may be because of the loss of water molecules that had been bound with hydroxyl groups present in tannin and in the voids. Nearly 21% decomposition takes place in the temperature range of 155–310°C. The third stage occurs in the temperature range of 310–800°C, in which the weight loss was 33%. The char yield was 40%. The thermal stability of MTR was higher than the VTR.

For the study on the kinetics of thermal degradation of MTR and VTR, we can select the isothermal ther-

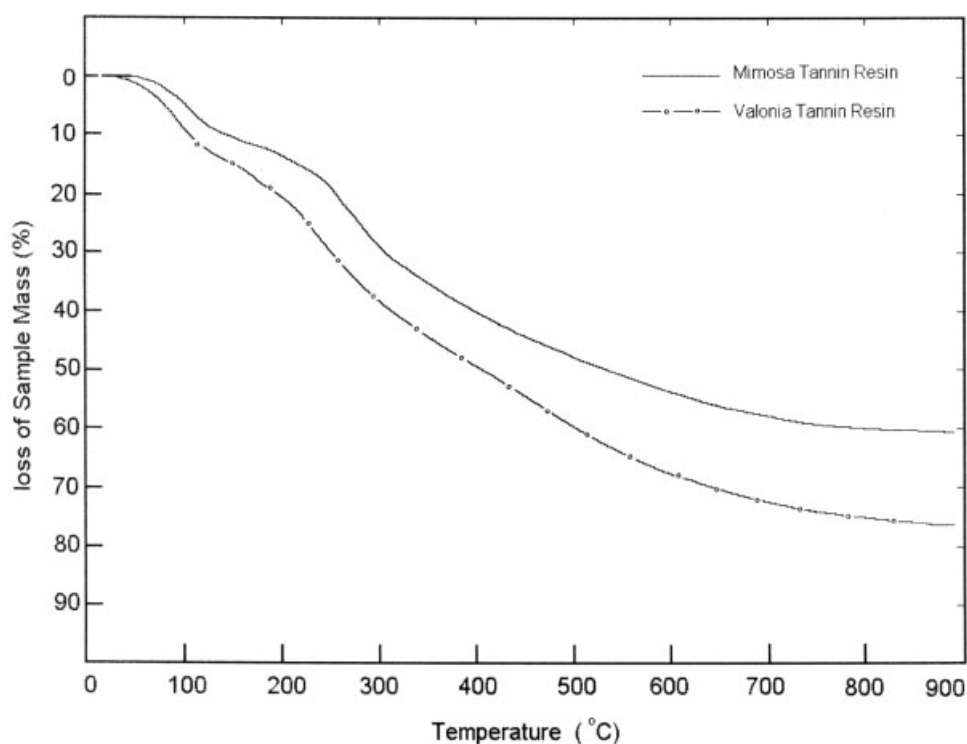


Figure 3 TGA curves of MTR and VTR.

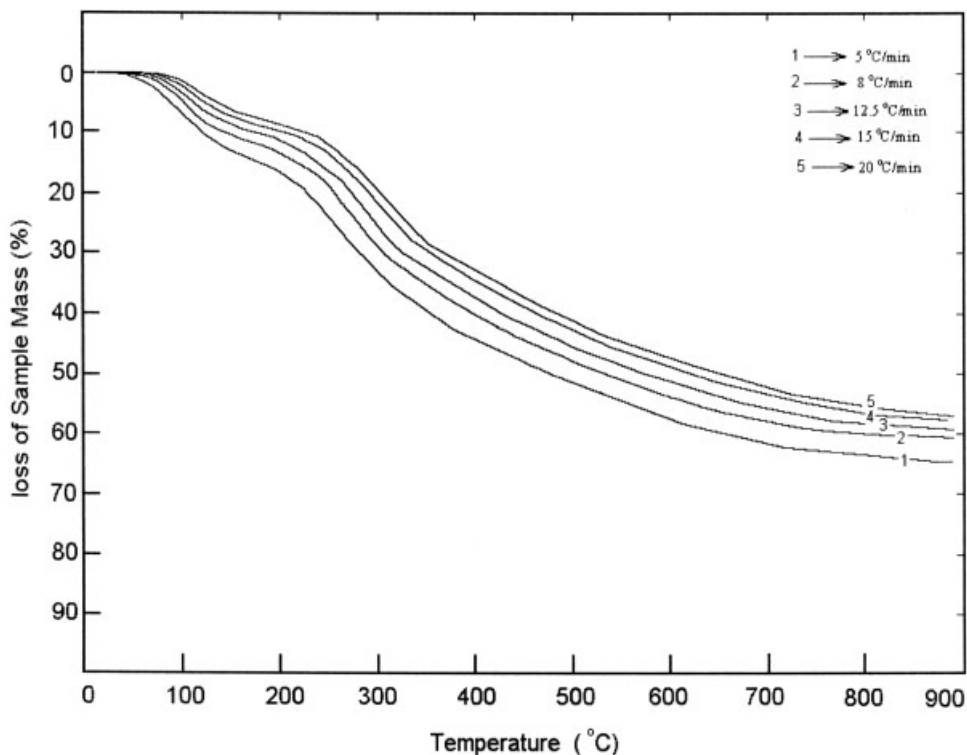


Figure 4 The thermal degradation curves of MTR at different heating rates.

mogravimetry (ITG) or the thermogravimetry (TG) at various heating rates.³⁸ ITG is superior to obtain an accurate activation energy for thermal degradation, although it is time-consuming. In the case of thermal degradation of materials, in which crosslinking due to the side groups, the TG at various heating rates is much more convenient than ITG for the investigation of thermal degradation kinetics. Therefore, in the present work, TG curves at various heating rates were obtained and the activation energies (ΔE_d) for thermal degradation of compounds were calculated by Ozawa's plot, which is a widely used method. Degradations were performed in the scanning mode, from 30 up to 900°C, under nitrogen flow (20 mL min⁻¹), at various heating rates (β : 5.0, 8.0, 12.5, 15.0, and 20.0°C min⁻¹). In Figure 4, the TGA thermograms of MTR are shown.

According to the method of Ozawa,³⁹ the apparent thermal decomposition activation energy, E_d , can be determined from the TGA thermograms under various heating rates, such as in Figure 4, and the following equation:

$$F_d = -\frac{R}{b} \left[\frac{d \log \beta}{d(1/T)} \right] \quad (1)$$

where R is the gas constant; b , a constant (0.4567); and β , the heating rate (°C/min). According to eq. (1), the activation energy of degradation can be determined

from the slope of the linear relationship between $\log \beta$ and $1/T$, as shown in Figure 5; the ΔE_d values for MTR and VTR are given in Table I. ΔE_d calculated from the Ozawa method is superior to other methods for complex degradation, since it does not use the reaction order in the calculation of the decomposition activa-

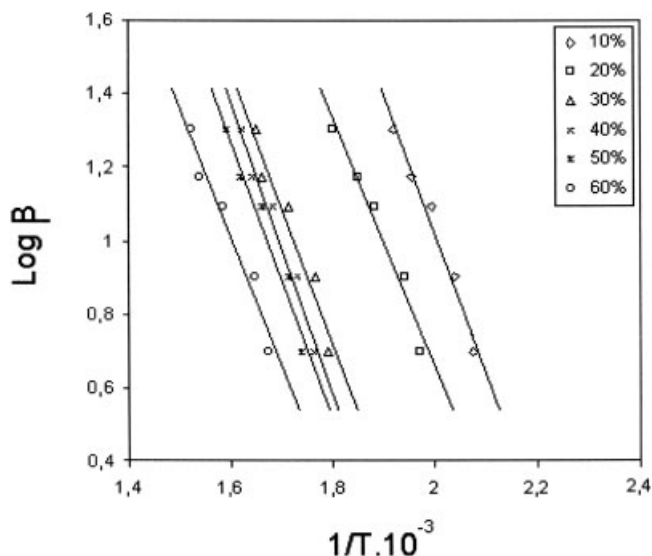


Figure 5 Ozawa's plots of logarithm of heating rate (β) versus reciprocal temperature ($1/T$) at different conversions for MTR.

TABLE I
The Apparent Activation Energies of Resins Under Thermal Degradation in N₂

Sample	Activation energy ΔE_a (kJ/mol)						Average
	10%	20%	30%	40%	50%	60%	
MTR	44.2	40.0	40.6	26.0	24.1	22.6	32.92
VTR	49.0	44.8	41.0	26.6	27.4	27.0	35.97

tion energy.⁴⁰ Therefore, ΔE_a calculated from the Ozawa method was superior to the former methods for complex degradation.

The glass transition (T_g) temperatures were determined by a Setaram 131 DSC. Samples of about 5–8 mg held in sealed aluminum crucibles and a heating rate of 20°C/min under a dynamic nitrogen flow (5 L h⁻¹) were used for the measurements. The differential scanning calorimetry (DSC) traces for the two resins are shown in Figure 6. In all cases, the curves are endothermic. The first point of instability on the curve has been taken as the glass transition temperature (T_g). From Figure 6, the T_g for VTR and MTR are estimated as 72 and 76°C, respectively. This estimation is debatable because the points of instability are not very pronounced. The more pronounced transformations, represented by the turning points on the DSC curves in Figure 6, has more to do with the chemical breakdown or evolution of moisture and formaldehyde in the resins. Data analysis was carried out with the

Setaram software package. The enthalpy changes (ΔH_p^d) and heat capacity ΔC_p during thermal degradation obtained from the DSC thermograms of polymers are given in Table II.

Mechanism of adsorption of metals onto MTR and VTR

The results of the adsorption of various metal ions onto MTR and VTR are given in Table III. It can be seen from Table III that the adsorption capacity of VTR is higher than MTR. This situation may be explained based on the VTR and MTR containing of different surface reactive groups such as catechol and pyrogallol groups to binding metal ions. VTR contains three adjacent hydroxyl groups for binding of metal ions, whereas B-ring of MTR contains two adjacent hydroxyl groups.

The mechanism by which metal ions are adsorbed onto different tannin resins has been a matter of considerable debate. Different studies have reached different conclusions. These include ion-exchange, surface adsorption, chemisorption, complexation, and adsorption-complexation. It is commonly believed that ion-exchange is most prevalent mechanism. Metals react with phenolic groups of the tannin resins to release protons with their anion sites to displace an existing metal. Based on the complex polyhydric phenolic nature of the MTR and VTR, a possible mechanism of ion exchange could be considered as divalent

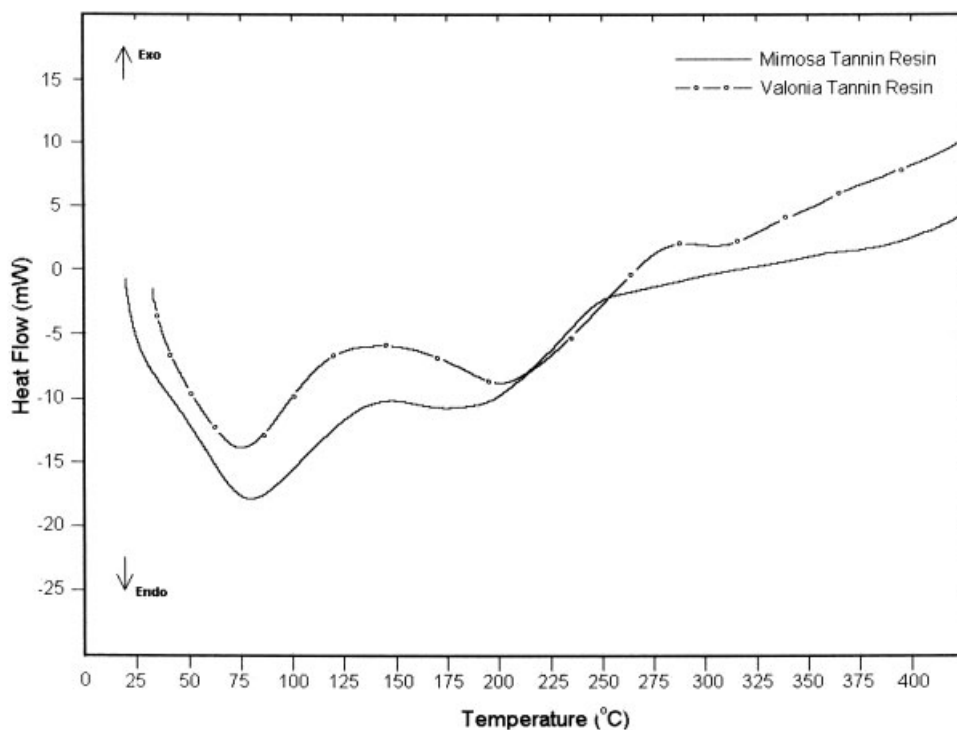


Figure 6 DSC curves of MTR and VTR.

TABLE II
Enthalpy Changes (ΔH_p^d) and Heat Capacity (ΔC_p) During Thermal Degradation Obtained from the DSC Thermograms of Resins

Sample	Onset point	Peak 1 top	Offset point	ΔH_p^d (J/g)	ΔC_p (J/g K)	Onset point	Peak 2 top	Offset point	ΔH_p^d (J/g)	ΔC_p (J/g K)
MTR	32.4	77.2	130.4	227.6	-13.5	144.1	180.0	224.4	116.1	-7.2
VTR	30.1	74.0	118.8	240.4	-16.2	150.2	194.4	256.8	166.2	-11.8

metal ion (M^{2+}) attaching itself to adjacent hydroxyl groups and oxyl groups, which could donate two pairs of electrons to metal ions, forming chelated compounds and releasing two hydrogen ions into solution.⁴¹

Other studies have found evidence that tannin resins take up metals by complexation, surface adsorption, and chemisorption.⁴²⁻⁴⁴ Hemingway⁴² concluded that the catechol or pyrogallol B-rings offer special opportunities for formation of metal complexes. Metals form complexes with the phenolics with two adjacent hydroxyls (catechols), and the presence of a third adjacent hydroxyl (pyrogallols) increases the stability of the complexes.⁴² The chemisorptive bond could be formed by sharing a pair of electrons, from the organic adsorbent, with metals. The organic adsorbent, containing S, N, O, Se, or P, are usually regarded as the reaction center for the chemisorption process. Natural tannin derivatives are oxygen-containing adsorbents; therefore, formation of metal-oxygen bond is possible.⁴⁴

Several studies support the general view that the reaction of metal ions, such as Cu and Fe, with tannin resin is one of chelate ring formation involving adjacent aromatic carboxylate $-\text{COOH}$ and phenolic $-\text{OH}$ groups or, less commonly, two adjacent $-\text{COOH}$ groups, which participate in ion-exchange reactions by binding metal ions with release of H^+ ions.^{41,43-46}

Surface adsorption is another mechanism by which metal ions may be bound to tannin resin. This mechanism is a surface reaction where a positively charged metal ion is attracted to a negatively charged surface without the exchange of ions or electrons.

TABLE III
Adsorbed Amount of Various Metals Ions onto MTR and VTR

Adsorbent	Adsorbed amount (mg/g)			
	Pb	Cu	Zn	Cd
MTR	64.88	36.83	28.68	16.81
VTR	98.50	43.17	37.62	36.81

Conditions: 75–100 μm particle size, 100 mg/L concentrations, 1 g/L dose, 150 rpm agitation for 3 h, 298 K temperature, and pH 4.

We believed that the adsorption mechanism may be partly a result of the ion exchange or complexation between the metal ions and phenolic groups on the MTR and VTR surfaces. Thus, the metal ions/tannin resins reaction may be represented in two ways as shown in Scheme 5.

CONCLUSIONS

Both mimosa tannin- and valonia tannin-formaldehyde condensation have been studied. Mimosa tannin and valonia tannin resin, which are obtained by the condensation reaction between formaldehyde and tannins, do not dissolve in water, whereas the natural tannin compounds dissolve in water. They were used as adsorbents for the removal of various metal ions from aqueous solutions. Ion exchange and complexation as possible adsorption mechanisms were proposed and discussed. Two tannin resins obtained were characterized by FTIR spectroscopy before and after adsorption of various metal ions. Also, two tannin resins were characterized by differential scanning calorimetry (DSC) and thermogravimetric analysis (TG). Thermal and kinetic data suggest that the two resins are highly stable, and may be used for the removal of metal ions at room temperature.

References

1. Nakano, Y.; Tanaka, M.; Nakamura, Y.; Konno, M. *J Chem Eng Jpn* 2000, 33, 747.
2. Schofield, P.; Mbugua, D. M.; Pell, A. N. *Animal Feed Sci Technol* 2001, 91, 21.
3. Bisanda, E. T. N.; Ogola, W. O.; Tesha, J. W. *Cem Concr Comp* 2003, 25, 593.
4. Steiner, P. R. In *Chemistry and Significance of Condensed Tannins*; Hemingway, R. W.; Karchesy, J. J., Eds.; Plenum Press: New York, 1989; pp 517.
5. Seeram, N.; Lee, R.; Hardy, M.; Heber, D. *Sep Purif Technol* 2005, 41, 49.
6. Madhan, B.; Muralidharan, C.; Jayakumar, R. *Biomaterials* 2002, 23, 2841.
7. Takahashi, T.; Yokoo, Y.; Inoue, T.; Ishii, A. *Food Chem Technol* 1999, 37, 545.
8. Kim, S.; Kim, H. J. *J Adhes Sci Technol* 2003, 17, 1369.
9. Christiansen, A. W.; Gollob, L. *J Appl Polym Sci* 1985, 30, 2279.
10. Park, B. D.; Riedl, B.; Hsu, E. W.; Shields, J. *Holz-Roh Werkstoff* 1998, 56, 155.
11. Garro-Galvez, J. M.; Riedl, B. *J Appl Polym Sci* 1997, 65, 399.

12. Lorenz, L. F.; Christiansen, A. W. *Ind Eng Chem Res* 1995, 34, 4520.
13. Pizzi, A. *Wood Adhesives Chemistry and Technology*, Vol. 1; Dekker: New York, 1983.
14. Broadhurst, R. B.; Jones, W. T. *J Sci Food Agric* 1978, 29, 788.
15. Price, M. L.; Butler, L. G. *J Agric Food Chem* 1977, 25, 1268.
16. Inoue, K. H.; Hagerman, A. E. *Anal Biochem* 1988, 169, 363.
17. Özacar, M.; Şengil, İ. A. *Water Res* 2000, 34, 1407.
18. Martinez, S. *Mater Chem Phys* 2002, 77, 97.
19. Zhan, X. M.; Zhao, X. *Water Res* 2003, 37, 3905.
20. Pizzi, A.; Scharfetter, H. O. *J Appl Polym Sci* 1978, 22, 1745.
21. Pizzi, A. *J Appl Polym Sci* 1978, 22, 2397.
22. Pizzi, A. *J Appl Polym Sci* 1979, 24, 1257.
23. Pizzi, A. *Int J Adhes Adhes* 1980, 1, 13.
24. Sowunmi, S.; Ebevele, R. O.; Peters, O.; Conner, A. H. *Polymer Int* 2000, 49, 574.
25. Haslam, E. *Plant Polyphenols, Vegetable Tannins Revisited*; Cambridge University Press: UK, 1989.
26. Niemetz, R.; Gross, G. G. *Phytochemistry* 2001, 58, 657.
27. Özacar, M.; Şengil, İ. A. *Colloids Surf A* 2003, 229, 85.
28. Garro-Galvez, J. M.; Fechtal, M.; Riedl, B. *Thermochim Acta* 1996, 274, 149.
29. Holopainen, T.; Alvilva, L.; Rainio, J.; Pakkanen, T. T. *J Appl Polym Sci* 1998, 69, 2175.
30. Lee, Y. K.; Kim, H. J.; Rafailovich, M.; Sokolov, J. *Int J Adhes Adhes* 2002, 22, 375.
31. Silverstein, R. M.; Webster, F. X. *Spectrometric Identification of Organic Compounds*, 6th ed.; Wiley: New York, 1998; pp 90, 91.
32. Garnier, S.; Pizzi, A.; Vorster, O. C.; Halasz, L. *J Appl Polym Sci* 2002, 86, 852.
33. Zhang, L. M.; Yin, D. Y. *J Appl Polym Sci* 1999, 74, 1662.
34. Özacar, M.; Şengil, İ. A. *J Hazard Mater* 2003, B100, 131.
35. Özacar, M.; Şengil, İ. A. *Turk J Eng Environ Sci* 2003, 27, 227.
36. Araña, J.; Rendón, E. T.; Doña Rodríguez, J. M.; Herrera Melián, J. A.; González Díaz, O.; Pérez Peña, J. *Chemosphere* 2001, 44, 1017.
37. Sekaran, G.; Thamizharasi, S.; Ramasami, T. *J Appl Polym Sci* 2001, 81, 1567.
38. Wendlandt, W. W. *Thermal Analysis*; Wiley: New York, 1986; p 57.
39. Ozawa, T. *Bull Chem Soc Jpn* 1965, 38, 1881.
40. Regnier, N.; Guibe, C. *Polym Degrad Stab* 1997, 55, 165.
41. Yu, L. J.; Shukla, S. S.; Dorris, K. L.; Shukla, A.; Margrave, J. L. *J Hazard Mater B* 2003, 100, 53.
42. Hemingway, R. W. In *Chemistry and Significance of Condensed Tannins*; Hemingway, R. W.; Karchesy, J. J., Eds.; Plenum Press: New York, 1989; p 299.
43. Bliss, E. D. In *Chemistry and Significance of Condensed Tannins*; Hemingway, R.W.; Karchesy, J. J.; Eds.; Plenum Press: New York, 1989; p 493.
44. Martinez, S.; Štern, I. *J Appl Electrochem* 2001, 31, 973.
45. Vázquez, G.; González-Álvarez, J.; Freire, S.; López-Lorenzo, M.; Antorrena, G. *Biores Technol* 2002, 82, 247.
46. Nakajima, A. *Talanta* 2002, 57, 537.